

Competition between ferroelectric and flexoelectric polarization in freely suspended smectic films

D. Schlauf¹, Ch. Bahr^{1,a}, V.K. Dolganov², and J.W. Goodby³

¹ Institute of Physical Chemistry, University Marburg, 35032 Marburg, Germany

² Institute of Solid State Physics, Russian Academy of Sciences, 142432 Chernogolovka, Moscow District, Russia

³ School of Chemistry, The University, Hull HU6 7RX, UK

Received 21 October 1998

Abstract. We report a detailed ellipsometric study of freely suspended films of chiral liquid-crystal compounds possessing smectic-A and smectic-C phases. In the temperature region between the smectic-A – smectic-C bulk and surface transitions, a discontinuous reconstruction of the tilt profile across the film is observed in the presence of a constant d.c. electric field. Comparison of the measured ellipsometric quantities with values calculated from model tilt profiles reveals a competition between a structure possessing a homogeneous tilt direction and large ferroelectric polarization and a structure with opposite tilt direction in the two film halves and large flexoelectric polarization.

PACS. 61.30.Gd Orientational order of liquid crystals; electric and magnetic field effects on order – 64.70.Md Transitions in liquid crystals

1 Introduction

Because of their layered structure, smectic liquid crystals can form films which are freely suspended across an opening in a thin glass or metal plate. The films consist of an integral number (adjustable between several hundred and only two) of molecular smectic layers which are arranged parallel to the two free surfaces. If a phase transition between smectic phases is approached from above, the layers at the surface transform into the low-temperature phase usually well above the bulk transition temperature (recent reviews are [1,2]). On further approaching the bulk transition temperature, the low-temperature phase grows into the interior of the film, in most cases *via* a series of layer-by-layer transitions. Finally, when the bulk transition temperature is reached, the complete film has adopted the structure of the low-temperature phase.

In the two simplest smectic phases, smectic-A (Sm-A) and smectic-C (Sm-C), each smectic layer is a two-dimensional liquid of orientationally ordered rodlike molecules, the mean direction of the long molecular axis, the director \mathbf{n} , being either parallel (Sm-A) or inclined by a tilt angle θ (Sm-C) with respect to the layer normal \mathbf{z} . Of particular interest are the properties of these phases if the constituent molecules are chiral: each layer of the Sm-C phase possesses then a ferroelectric spontaneous polarization \mathbf{P}_s directed along $\mathbf{n} \times \mathbf{z}$ [3]. The presence of \mathbf{P}_s is essentially a property of the single smectic layer, as was shown already in the first work [4,5] on freely suspended


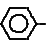
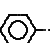
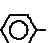

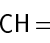
Sm-C films, where \mathbf{P}_s was measured and used to align \mathbf{n} by an external d.c. electric field in films as thin as three or two smectic layers.

If freely suspended films of a compound possessing Sm-A and Sm-C phases are prepared, the Sm-C phase appears in the surface layers usually at a temperature 10 to 20 K above the bulk Sm-A – Sm-C transition temperature. With decreasing temperature, the two tilted surface domains grow continuously into the interior of the film as was observed for a number of compounds and various film thicknesses [6–9]. In medium thick films (30 to 50 layers), one can expect in the temperature range between the Sm-A – Sm-C surface and bulk transitions the occurrence of structures with high θ values ($\approx 30^\circ$) at the surfaces and $\theta \approx 0^\circ$ in the interior. Since the direction of \mathbf{n} in such a structure changes rapidly over a small distance of almost molecular dimension, there is a strong bend deformation of the \mathbf{n} field which may result in the occurrence of a flexoelectric polarization \mathbf{P}_f [10]. The direction of \mathbf{P}_f is along $(\nabla \times \mathbf{n}) \times \mathbf{n}$, *i.e.*, \mathbf{P}_f is within the tilt plane (the plane containing \mathbf{z} and \mathbf{n}) and thus perpendicular to \mathbf{P}_s .

Depending on the amount of P_f and P_s , the occurrence of \mathbf{P}_f may result, in the presence of a constant d.c. electric field, in a reorientation of the tilt plane in a freely suspended film by 90° . Recent optical reflectivity measurements indicated that such a reorientation indeed occurs in films of suitable thickness [11]. We present here a detailed ellipsometric study which confirms the assumptions about the occurring structures made in [11]. Our results show unambiguously, that a structure in which

^a e-mail: bahr@mail.ner.uni-marburg.de

Table 1. Compounds under investigation

MB10OBC: Sm-C 49.5°C Sm-A 63°C isotropic
$C_{10}H_{21}COO$ -  -  -COO - CH ₂ - CH(CH ₃) - C ₂ H ₅
MB12OBC: Sm-C 50°C Sm-A 64°C isotropic
$C_{12}H_{25}COO$ -  -  -COO - CH ₂ - CH(CH ₃) - C ₂ H ₅
NOBAMBC: Sm-C 92°C Sm-A 116°C isotropic
$C_9H_{19}O$ -  -CH=N-  -CH=CH - COO - CH ₂ - CH(CH ₃) - C ₂ H ₅

the directions of the molecular tilt and \mathbf{P}_s is the same in all layers (*i.e.*, the usual structure adopted in an external d.c. field) can transform, accompanied by a simultaneous reorientation of the tilt plane by 90°, into a bend structure with opposite tilt directions in the two halves of the film.

2 Experimental

We report here results obtained on three liquid-crystal compounds. The molecular structures and bulk transition temperatures are given in Table 1. The compound NOBAMBC is a homolog of the well-known compound DOBAMBC [3], MB10OBC and MB12OBC are homologs of the compound MB8OBC which has been studied in detail in [8,9]. The phase sequence for all compounds is isotropic – Sm-A – Sm-C.

Freely suspended films are drawn in the Sm-A phase using a rectangular, variable-area frame described in [12]. The typical film area is $5 \times 10 \text{ mm}^2$. The beam of a HeNe-Laser transmits the film under an angle of incidence of 45°. Using a null-ellipsometer (details can be found in [13]) we determine the quantities Δ and Ψ which describe the state of polarization of the transmitted light. As usual, Δ corresponds to the phase difference between the *p*- and *s*-polarized components of the transmitted light, $\Delta = \delta_p - \delta_s$, and Ψ is related to the amplitudes of the *p*- and *s*-components, $\tan \Psi = |E_p|/|E_s|$. The polarization of the incident light is described by $\Delta = 0$ and $\Psi = 45^\circ$.

A weak d.c. electric field (8 V/cm) is applied in the film plane perpendicular to the plane of incidence (the plane containing the film normal and the incident laser beam). Values of Δ and Ψ are continuously collected while the temperature is changed at a slow constant rate (typically between 1 and 2 K/h). At least two, in most cases four measurement runs are conducted: we start with a cooling run which is followed by a heating run, then the polarity of the d.c. field is inverted and again a cooling and a heating run are recorded.

The d.c. field aligns the electric polarization of the film. If only a ferroelectric polarization \mathbf{P}_s would be present,

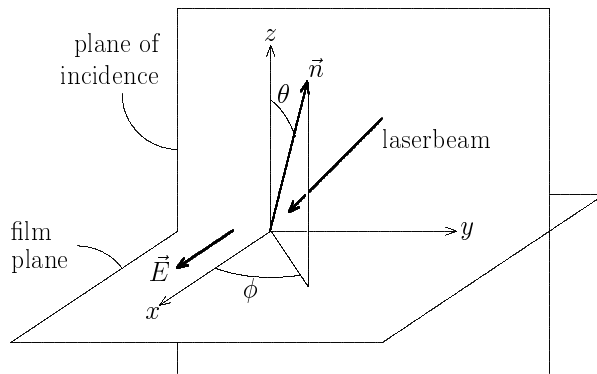


Fig. 1. Experimental geometry: \mathbf{n} is the director, the film normal and smectic layer normal is along z , the laser beam is within the yz -plane and hits the film plane with an angle of incidence of 45° , the applied d.c. field is along $\pm x$, the tilt magnitude is given by the angle θ , the tilt direction is specified by the angle ϕ (*e.g.*, $\phi = 270^\circ$ corresponds to a tilt direction within the plane of incidence and away from the incident laser beam). We have denoted the field direction shown above as the +-polarity, all three compounds under investigation tilt with this polarity in their bulk Sm-C phase in the direction $\phi = 270^\circ$.

\mathbf{n} would be always within the plane of incidence and only two tilt directions (away from or towards the incident beam) would be possible. In our previous papers [8,9,13] we have denoted the values of Δ belonging to these two tilt directions by subscripts “+” or “-”. In the present study we use these subscripts just to denote the polarity of the applied d.c. field (see Fig. 1), independently of the resulting tilt direction. The tilt direction will be specified in the following by the value of the azimuthal angle ϕ as illustrated in Figure 1.

3 Results and discussion

Figure 2 shows the results for a 33-layer film of MB10OBC. The Sm-A – Sm-C surface transition occurs (in films

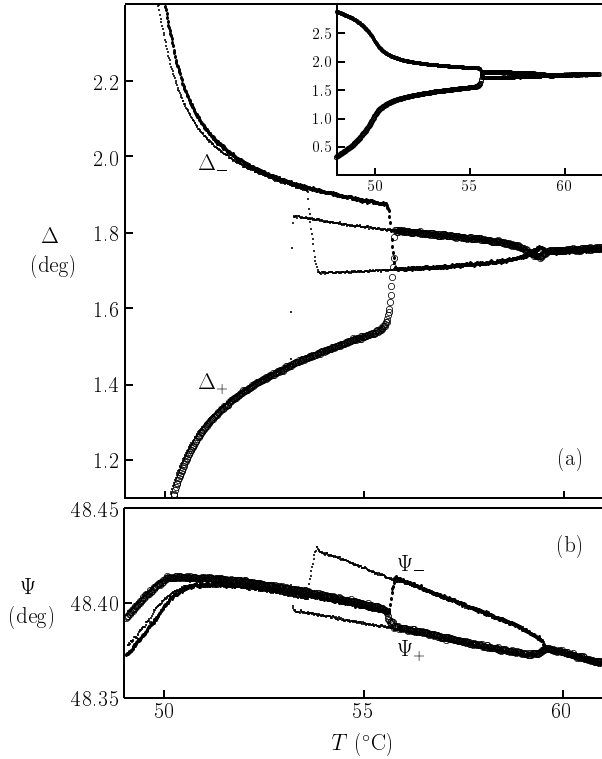


Fig. 2. Temperature dependence of the ellipsometric quantities Δ (a) and Ψ (b) for a 33-layer film of MB10OBC ($T_{\text{bulk}} = 49.5$ °C, $T_{\text{surf}} = 59.5$ °C); open circles: heating with +polarity of applied d.c. field, small dots: heating run with –polarity, tiny dots: corresponding cooling runs. The abrupt change of Δ and Ψ at 56 °C/53 °C (heating/cooling) indicates the change from the C-structure at higher temperatures to the S-structure at lower temperatures (see text and Fig. 5).

thicker than 8 layers) at 59.5 °C, the Sm-A – Sm-C bulk transition temperature of this compound amounts to 49.5 °C. Below the bulk transition temperature and a few degrees above, the usual behavior of Δ (described in [8,9]) is observed: the tilt direction is within the plane of incidence and, depending on the field polarity, either towards or away from the incident beam; in this geometry the difference between Δ_+ and Δ_- is a measure of the amount of θ . It is obvious that some degrees above the bulk transition temperature a discontinuous structural change occurs, as is indicated by the jumps of the Δ and Ψ values. There is a pronounced thermal hysteresis of 2–3 K between heating and cooling runs confirming the discontinuous character of the transition to the new structural state occurring at higher temperatures.

Of particular interest is the behavior of Ψ . If the tilt direction would be in all layers of the film exactly within the plane of incidence, one would obtain $\Psi_+ = \Psi_-$. This is experimentally observed above the surface transition (this is trivial since $\theta = 0$ in all layers) and below the temperature where the discontinuous change of the Δ and Ψ values occurs [14]. In the temperature region in between, a pronounced difference between Ψ_+ and Ψ_- is obtained. Any structure in which the tilt plane in all layers coincides

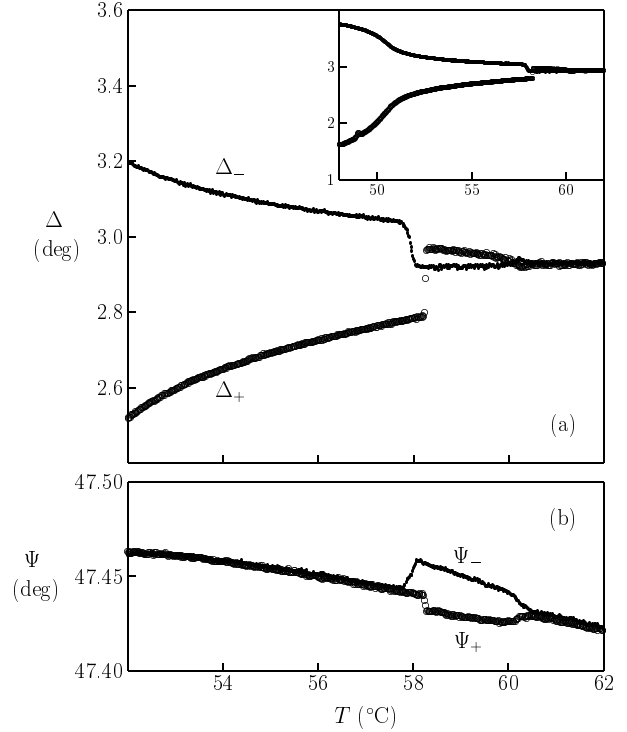


Fig. 3. Temperature dependence of Δ and Ψ for a 25-layer film of MB12OBC ($T_{\text{bulk}} = 50$ °C, $T_{\text{surf}} = 60$ °C); only heating runs are shown (see caption of Fig. 2).

with the plane of incidence is not compatible with this result, regardless whether the tilt direction is towards or away from the incident beam. Thus, the new state must be characterized by a structure in which the tilt direction is at least in some layers not perpendicular to the applied field, *i.e.*, the alignment of the tilt direction is not solely controlled by the ferroelectric polarization.

Measurements on the two other compounds, MB12OBC and NOBAMBC, yield essentially the same results (see Figs. 3 and 4). Optical reflectivity measurements [11] on freely suspended films of NOBAMBC yielded sudden changes of the reflectivity in the temperature range between the bulk and surface Sm-A – Sm-C transition which can be identified with the sudden changes of the ellipsometric quantities Δ and Ψ observed here. According to [11], the reflectivity changes result from the discontinuous change between two structures which differ in their tilt profile across the film which is either S- or C-shaped (see Fig. 5). The S-structure occurs below and a few degrees above the bulk transition temperature. There is a large total magnitude of the ferroelectric polarization \mathbf{P}_s since the tilt direction is the same in all layers. Although there is a bend deformation and thus a flexoelectric polarization \mathbf{P}_f in each half of the film, the net magnitude of \mathbf{P}_f is zero because of the S-shaped \mathbf{n} field. At higher temperatures, the new state occurs where the \mathbf{n} profile has the shape of a C; in this structure, the net magnitude of \mathbf{P}_s of the film is zero (because the tilt directions in the two film halves are opposite) but there is a large total magnitude of \mathbf{P}_f .

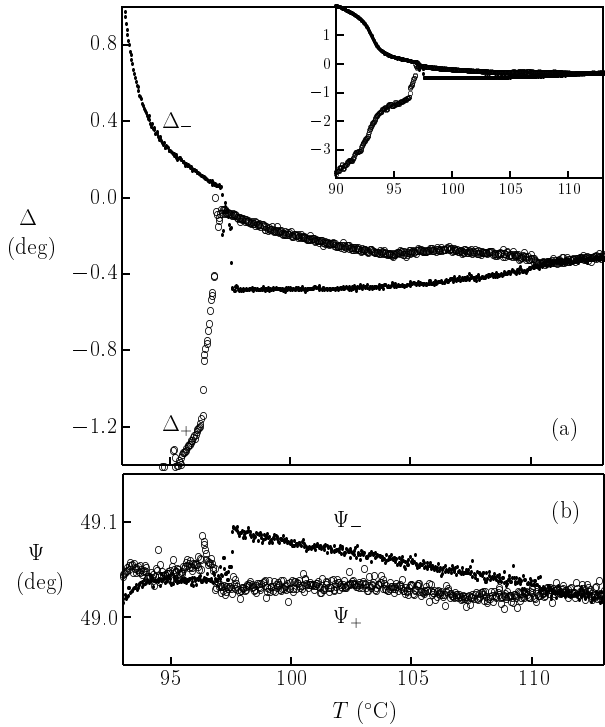


Fig. 4. Temperature dependence of Δ and Ψ for a 32-layer film of NOBAMBC ($T_{\text{bulk}} = 92^\circ\text{C}$, $T_{\text{surf}} = 110^\circ\text{C}$); only heating runs are shown (see caption of Fig. 2).

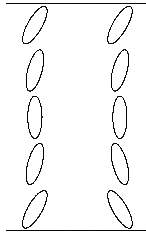


Fig. 5. Schematic drawings of the tilt profiles of the S-structure (left) and the C-structure (right). In the S-structure, ϕ has the same value in all layers, in the C-structure ϕ changes by 180° in the middle of the film.

In the following we calculate the qualitative temperature dependence of Δ and Ψ for model films possessing S- and C-structures as shown in Figure 5. This calculation starts considering the transmission matrix T , which relates the electric field of the light which has passed the film to the field of the incident light:

$$\begin{pmatrix} E_{tp} \\ E_{ts} \end{pmatrix} = \begin{pmatrix} T_{pp} & T_{ps} \\ T_{sp} & T_{ss} \end{pmatrix} \begin{pmatrix} E_{ip} \\ E_{is} \end{pmatrix}. \quad (1)$$

Here, E_{tp} , E_{ts} , E_{ip} , E_{is} are the p - and s -polarized components of the transmitted and incident light. Note that all quantities in equation (1) are complex possessing an absolute value (amplitude) and an argument (phase). If for the incident light $E_{ip} = E_{is}$, the values Δ and Ψ , which are measured by ellipsometry, can be related to the elements

of T :

$$\Delta = \arg \left(\frac{T_{pp} + T_{ps}}{T_{sp} + T_{ss}} \right) \quad (2)$$

$$\tan \Psi = \left(\left| \frac{T_{pp} + T_{ps}}{T_{sp} + T_{ss}} \right| \right). \quad (3)$$

When the film can be treated as a uniaxial optical system with its optical axis either normal to the film plane or tilted within the plane of incidence, the off-diagonal elements T_{ps} and T_{sp} vanish and T_{pp} and T_{ss} can be calculated using Fresnel coefficients and considering the corresponding phase shifts as described in [13]. However, to calculate Δ and Ψ for structures as shown in Figure 5, we treat the film as a multilayer system in which each layer is assumed as uniaxial but the optical axis of each layer is allowed to take any value of tilt magnitude θ and tilt direction ϕ . We calculate T using the 4×4 matrix formalism [15,16] as described in the Appendix.

Each layer of the film enters in the calculation with its extraordinary and ordinary refractive index n_e (or n_{\parallel}) and n_o (or n_{\perp}), layer thickness d , tilt magnitude θ , and tilt direction ϕ . For our model film we set the thickness to 30 layers and assume for each layer $n_e = 1.6$, $n_o = 1.5$, and $d = 3$ nm (which are just typical values of liquid-crystal compounds). We further assume that the temperature dependence of θ in the two surface layers is described by a power-law: $\theta_{\text{surf}} \propto (\Delta T_{\text{surf}})^{0.25}$ where ΔT_{surf} corresponds to the temperature difference to the surface transition temperature. According to mean-field theory, the tilt magnitude (or order parameter) profile across the film, which is induced by the tilt in the surface layers, has the shape of a cosh-function [17,18]:

$$\theta(z) = \theta_{\text{surf}} \frac{\cosh[(2z - L)/2\xi]}{\cosh(L/2\xi)}. \quad (4)$$

Here, L is the thickness of the film and z the distance from one of the surfaces. The value of the correlation length ξ determines, how far the tilted surface region penetrates into the interior of the film; we let ξ diverge as $\xi \propto (\Delta T_{\text{bulk}})^{-0.6}$ where ΔT_{bulk} is the temperature difference to the bulk transition. Our aim here is not to confirm the exact shape of the tilt profile or the values of the critical exponents above, we just want to get a simple qualitative model possessing a surface tilt which grows into the interior of the film with decreasing temperature.

With the temperature dependent θ profile described above, we calculate Δ and Ψ for the S- and C-structures shown in Figure 5 with the tilt plane being either parallel or perpendicular to the plane of incidence. For each orientation of the tilt plane, we further allow the two possible tilt directions, opposite to each other, inside the plane. As shown in Figure 6, the experimentally observed behavior of Δ and Ψ can be explained assuming a discontinuous change between S- and C structures with a simultaneous rotation of the tilt plane by 90° . Especially the difference between Ψ_+ and Ψ_- observed at higher temperatures (see Figs. 2-4) is well reproduced assuming the occurrence of

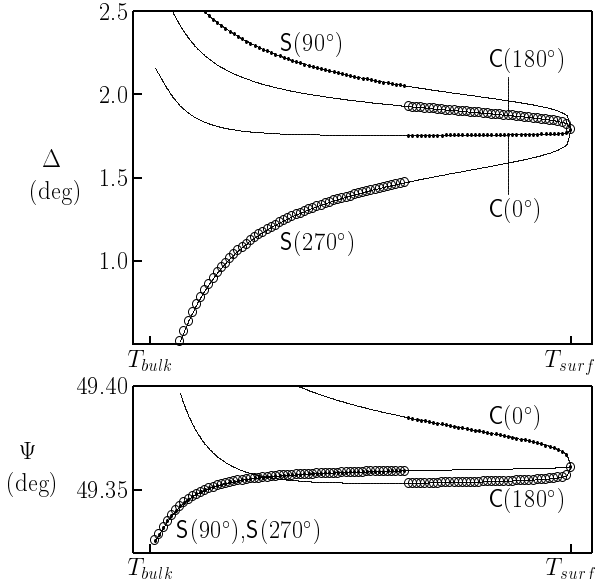


Fig. 6. Calculated temperature dependence of Δ and Ψ for S- and C-structures of a model film (see text), the numbers give the value of the tilt direction ϕ (for the C-structures, in which ϕ changes by 180° in the middle of the film, the value of ϕ refers to the upper half of the film, *i.e.*, the half which is facing the incident laser beam). The experimental behavior is qualitatively reproduced if we assume that C-/S-structures are stable at higher/lower temperatures and that the +-polarity of the applied d.c. field corresponds to the S(270°)- and C(180°)-structures (open circles) and the --polarity to the corresponding structures with opposite tilt direction (small dots).

the C-structure in this temperature range. Our ellipsometric measurements thus completely confirm the structures proposed in [11].

The transition from the C- to the S-structure in an external d.c. field occurs when the total magnitude of \mathbf{P}_s of the S-structure exceeds the total magnitude of \mathbf{P}_f of the C-structure. The temperature of this transition shows a characteristic dependence on the film thickness. As can be seen in Figure 7, the S - C transition temperature decreases with increasing film thickness. This behavior can be qualitatively understood by comparing the temperature dependencies of \mathbf{P}_f and \mathbf{P}_s which result from equation (4). The flexoelectric polarization of a bend deformation is in first approximation proportional to the change of the \mathbf{n} orientation per unit length along the appropriate direction [19], for a C-structure as shown in Figure 5 we can write $|P_f| = C_f |(\partial\theta/\partial z)|$ where C_f describes the strength of the coupling between the polarization and the bend deformation and depends on the molecular structure. For the total magnitude of \mathbf{P}_f of a film possessing the C-like tilt profile we get

$$|P_f| = C_f \int_0^L \left| \left(\frac{\partial\theta}{\partial z} \right) \right| dz. \quad (5)$$

Equation (5) is just a crude approximation, because it is based only on the variation of the tilt magnitude θ , it does not take into account the change of the tilt direction

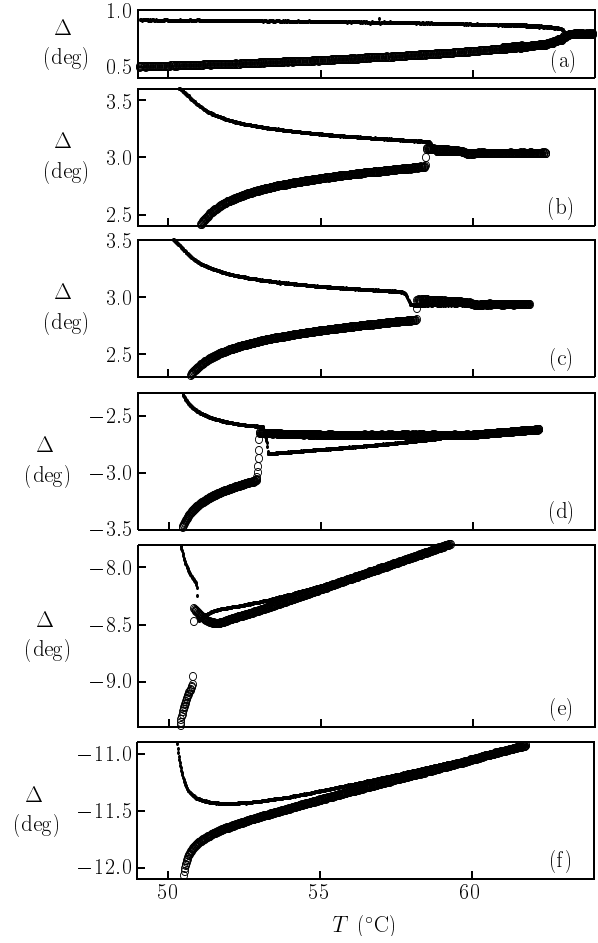


Fig. 7. Temperature dependence of Δ for various films of MB12OBC, film thicknesses are: 3 (a), 24 (b), 25 (c), 49 (d), 146 (e), and 312 layers (f); open symbols: +-polarity, small dots: --polarity, only heating runs are shown.

ϕ which is present in the C-structure in the middle of the film. The ferroelectric polarization is, in first approximation, proportional to the tilt magnitude, $P_s = C_s \theta$ with C_s being the appropriate coupling constant which depends as C_f on the molecular structure. The total magnitude of \mathbf{P}_s of a film possessing the S-like tilt profile is thus

$$|P_s| = C_s \int_0^L \theta(z) dz. \quad (6)$$

In a film of given thickness, the ratio $|P_f|/|P_s|$ decreases with decreasing temperature for two reasons: First, with decreasing temperature more layers of the film become tilted and inside each layer θ increases, resulting in a strong increase of $|P_s|$ near the bulk transition temperature. Secondly, with decreasing temperature $|P_f|$ decreases because the θ variation from layer to layer becomes less pronounced. The temperature, at which $|P_f| = |P_s|$, increases with decreasing film thickness because in thin films the state, where θ is of nearly the same magnitude in outer and inner layers and $|P_f|$ becomes small, is reached at a higher temperature compared to thicker films. In films thinner than about eight layers, we do not observe,

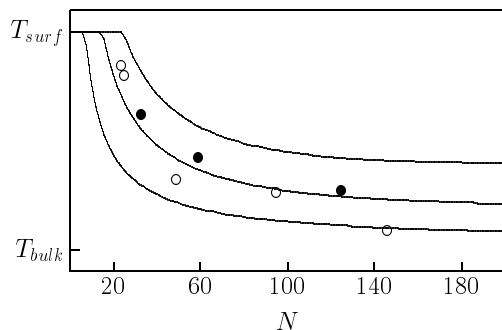


Fig. 8. Temperature of the C – S transition as a function of layer thickness; circles: experimental values (from heating runs) for MB10OBC (closed) and MB12OBC (open), solid lines: calculated values for model films, the difference between the three curves consists in the magnitude of the ratio C_f/C_s (see text) which was varied as $1 : \frac{1}{2} : \frac{1}{3}$ from the bottom to the top.

for the compounds studied here, an indication of the C-structure: obviously, in thin films $|P_f|$ is even just below the surface transition smaller than $|P_s|$. Figure 8 shows the qualitative dependence of the S – C transition temperature on the film thickness resulting from equations (4-6). There is a reasonable agreement with our experimental data. If the films are thicker than 100 layers, the behavior becomes more complicated. As shown in Figure 7e for a 146-layer film of MB12OBC, there is still a discontinuous change from the S-structure to a probably C-like structure but immediately above the transition there is a crossing of the Δ_+ and Δ_- curves which is not compatible with a C-structure as shown in Figure 5. In very thick films the C-structure does not seem to appear. Any discontinuous change has vanished, and Δ shows a similar dependence on temperature and field polarity as in very thin films (compare Figs. 7a and 7f). However, the difference between Δ_+ and Δ_- near the surface transition seems to be in very thick films smaller than in very thin films. These observations can be explained if we assume that in very thick films the two surfaces are “decoupled”. The external d.c. field then aligns at each surface the vector of the total polarization $\mathbf{P}_s + \mathbf{P}_f$ which leads to a different orientation of the tilt plane at each surface (in thin films such a variation of the tilt plane orientation across the film costs additional elastic energy and might be therefore suppressed in favor of the S- or C-structures in which the tilt plane is the same in all layers). If \mathbf{P}_s is large enough, the tilt orientation and the resulting Δ values will then appear similar to the case of the simple S-like structures.

The C-structure can be observed, of course, only for compounds possessing a large enough flexoelectric coupling constant C_f or a very small ferroelectric coupling constant C_s ; studies of chiral-racemic systems, in which C_s can be varied *via* the enantiomeric excess, would offer a possibility to check these assumptions. Concerning the compounds under investigation, there is some indication that the ratio C_f/C_s is smaller in MB10OBC compared to MB12OBC: the S – C transition temperatures are higher for MB10OBC (Fig. 8) and the Δ values in very thick films of MB10OBC appear to be less influenced by a flexoelec-

tric polarization compared to MB12OBC. Furthermore, in MB8OBC the C-structure does not appear [20], regardless of the film thickness. Thus, there seems to be a tendency for C_f to decrease with decreasing molecular length.

Finally, we would like to note that the occurrence of the C-structure can easily lead to erroneous interpretations of ellipsometric studies of freely suspended films. Especially in thicker films the Sm-A – Sm-C surface transition can be hard to detect: in an earlier study [21] we obtained from first measurements of MB12OBC Δ_+ and Δ_- curves, which were almost undistinguishable in the temperature range above the Sm-A – Sm-C bulk transition. This observation led us to the conclusion, that thick films of MB12OBC do not possess tilted surface layers, which is certainly wrong as is clearly shown by the present measurements.

4 Conclusion

We have reported ellipsometric measurements of chiral compounds possessing Sm-A and Sm-C phases. Our results show that for suitable compounds in the temperature range between the Sm-A – Sm-C bulk and surface transitions, the orientation of the molecules in an external d.c. electric field is determined not only by the ferroelectric polarization but also by a flexoelectric polarization which results from the strong variation of the tilt angle magnitude θ across the film. Near the surface transition and a few degrees below, where this θ variation is especially pronounced, the behavior is governed by the flexoelectric polarization: the tilt profile across the film has the shape of a C and the tilt plane is parallel to the applied field. At lower temperatures near the bulk transition, where the interior layers are also tilted to some extent, the ferroelectric polarization becomes predominant: the structure changes to a S-shaped tilt profile with the tilt plane perpendicular to the applied field.

The occurrence of the C-structure depends on the film thickness. It does not occur in very thin films because the difference of the tilt magnitude θ between surface and interior layers is not pronounced enough to produce a large flexoelectric polarization. With increasing film thickness, the temperature range of the C-structure, which is in thin films restricted to a small temperature interval just below the Sm-A – Sm-C surface transition, grows at the expense of the range of the S-structure until the C – S transition temperature is close to the Sm-A – Sm-C bulk transition. In very thick films a discontinuous C – S transition does not occur, the tilt direction in each part of the film is determined by the sum $\mathbf{P}_s + \mathbf{P}_f$ and can vary continuously with temperature because the molecular orientations at the two film surfaces do not influence each other.

This work was supported in part by the Deutsche Forschungsgemeinschaft (grant no. Ba1048/5) and the Fonds der Chemischen Industrie. Ch. B. is grateful to the Deutsche Forschungsgemeinschaft for a Heisenberg-Fellowship. V. D. thanks the Russian Fund for Fundamental Research (98-02-16639).

Appendix

Here we give the details of the calculation of the ellipsometric quantities Δ and Ψ for the model films described above. The film is considered as a stack of optically uniaxial layers which possess refractive indices n_{\perp} and n_{\parallel} (the values may differ from layer to layer but are assumed to stay constant inside each layer). The orientation of the optical axis of each layer is described by angles θ and ϕ as in Figure 1. The light, with wavelength λ , is incident from an ambient medium with refractive index n_0 (in our case air with $n_0 = 1$) onto the film with an angle θ_0 to the film normal.

The differential change of the electromagnetic field along the z direction inside each layer can be described by a 4×4 matrix, the differential propagation matrix D [16, 22]. D gives the partial derivatives ($\partial/\partial z$) of the field components $E_{x,y}, H_{x,y}$ (to avoid confusion with indices, the imaginary unit ($\sqrt{-1}$) is in the following designated by j):

$$\frac{\partial}{\partial z} \begin{pmatrix} E_x \\ H_y \\ E_y \\ -H_x \end{pmatrix} = -j \frac{2\pi}{\lambda} D \begin{pmatrix} E_x \\ H_y \\ E_y \\ -H_x \end{pmatrix}. \quad (7)$$

For a uniaxial layer, the matrix D has the elements [23]

$$D = \begin{pmatrix} D_{11} & D_{12} & D_{13} & 0 \\ D_{21} & D_{22} & D_{23} & 0 \\ 0 & 0 & 0 & 1 \\ D_{41} & D_{42} & D_{43} & 0 \end{pmatrix}, \quad (8)$$

with:

$$D_{11} = -\frac{\Delta\epsilon \sin\theta \cos\theta \sin\phi}{\epsilon_{33}} X, \quad (9)$$

$$D_{12} = 1 - \frac{X^2}{\epsilon_{33}}, \quad (10)$$

$$D_{13} = \frac{\Delta\epsilon \sin\theta \cos\theta \cos\phi}{\epsilon_{33}} X, \quad (11)$$

$$D_{21} = \epsilon_{\perp} \frac{\epsilon_{\parallel} - \Delta\epsilon \sin^2\theta \cos^2\phi}{\epsilon_{33}}, \quad (12)$$

$$D_{22} = D_{11}, \quad (13)$$

$$D_{23} = -\epsilon_{\perp} \frac{\Delta\epsilon \sin^2\theta \sin\phi \cos\phi}{\epsilon_{33}} X, \quad (14)$$

$$D_{41} = D_{23}, \quad (15)$$

$$D_{42} = D_{13}, \quad (16)$$

$$D_{43} = \epsilon_{\perp} \frac{\epsilon_{\parallel} - \Delta\epsilon \sin^2\theta \sin^2\phi}{\epsilon_{33}} - X^2, \quad (17)$$

$$\epsilon_{33} = \epsilon_{\perp} + \Delta\epsilon \cos^2\theta, \quad (18)$$

$$\Delta\epsilon = \epsilon_{\parallel} - \epsilon_{\perp}, \quad (19)$$

$$X = n_0 \sin\theta_0, \quad (20)$$

$$\epsilon_{\perp} = n_{\perp}^2, \quad (21)$$

$$\epsilon_{\parallel} = n_{\parallel}^2. \quad (22)$$

The total change of the electromagnetic field caused by a layer of finite thickness d can again be represented by a 4×4 matrix, the layer transfer matrix L , which is obtained by integrating equation (7). Usually this has to be done numerically. For our case of uniaxial layers with constant (independent of z) optical properties in each layer, an analytical solution exists [23], L can be directly calculated from D :

$$L = \beta_0 I + \beta_1 D + \beta_2 D^2 + \beta_3 D^3, \quad (23)$$

with I being the 4×4 unit matrix and

$$\begin{aligned} \beta_0 = & -l_2 l_3 l_4 \frac{f_1}{(l_1 - l_2)(l_1 - l_3)(l_1 - l_4)} \\ & - l_1 l_3 l_4 \frac{f_2}{(l_2 - l_1)(l_2 - l_3)(l_2 - l_4)} \\ & - l_1 l_2 l_4 \frac{f_3}{(l_3 - l_1)(l_3 - l_2)(l_3 - l_4)} \\ & - l_1 l_2 l_3 \frac{f_4}{(l_4 - l_1)(l_4 - l_2)(l_4 - l_3)}, \end{aligned} \quad (24)$$

$$\begin{aligned} \beta_1 = & (l_2 l_3 + l_2 l_4 + l_3 l_4) \frac{f_1}{(l_1 - l_2)(l_1 - l_3)(l_1 - l_4)} \\ & + (l_1 l_3 + l_1 l_4 + l_3 l_4) \frac{f_2}{(l_2 - l_1)(l_2 - l_3)(l_2 - l_4)} \\ & + (l_1 l_2 + l_1 l_4 + l_2 l_4) \frac{f_3}{(l_3 - l_1)(l_3 - l_2)(l_3 - l_4)} \\ & + (l_1 l_2 + l_1 l_3 + l_2 l_3) \frac{f_4}{(l_4 - l_1)(l_4 - l_2)(l_4 - l_3)}, \end{aligned} \quad (25)$$

$$\begin{aligned} \beta_2 = & -(l_2 + l_3 + l_4) \frac{f_1}{(l_1 - l_2)(l_1 - l_3)(l_1 - l_4)} \\ & - (l_1 + l_3 + l_4) \frac{f_2}{(l_2 - l_1)(l_2 - l_3)(l_2 - l_4)} \\ & - (l_1 + l_2 + l_4) \frac{f_3}{(l_3 - l_1)(l_3 - l_2)(l_3 - l_4)} \\ & - (l_1 + l_2 + l_3) \frac{f_4}{(l_4 - l_1)(l_4 - l_2)(l_4 - l_3)}, \end{aligned} \quad (26)$$

$$\begin{aligned} \beta_3 = & \frac{f_1}{(l_1 - l_2)(l_1 - l_3)(l_1 - l_4)} \\ & + \frac{f_2}{(l_2 - l_1)(l_2 - l_3)(l_2 - l_4)} \\ & + \frac{f_3}{(l_3 - l_1)(l_3 - l_2)(l_3 - l_4)} \\ & + \frac{f_4}{(l_4 - l_1)(l_4 - l_2)(l_4 - l_3)}, \end{aligned} \quad (27)$$

$$f_i = \exp[-j(2\pi/\lambda)l_i d], \quad (28)$$

$$l_{1,2} = \pm \sqrt{\epsilon_{\perp} - X^2}, \quad (29)$$

$$l_{3,4} = -\frac{\epsilon_{13}}{\epsilon_{33}}X \pm \frac{\sqrt{\epsilon_{\perp}\epsilon_{\parallel}}}{\epsilon_{33}} \times \left[\epsilon_{33} - \left(1 - \frac{\Delta\epsilon}{\epsilon_{\parallel}} \sin^2 \theta \cos^2 \phi\right) X^2 \right]^{1/2}, \quad (30)$$

$$\epsilon_{13} = \Delta\epsilon \sin \theta \cos \theta \sin \phi. \quad (31)$$

Then, the total transfer matrix P of the film is calculated by multiplying all layer transfer matrices L_i , *i.e.*, for a film consisting of N layers

$$P = \prod_{i=1}^N L_i. \quad (32)$$

The transfer matrix P obtained in this way relates the electric field at the film surface facing the incident beam, *i.e.*, the field of incident and reflected light with p - and s -polarized components $E_{ip}, E_{is}, E_{rp}, E_{rs}$, with the electric field at the other surface of the film, *i.e.*, the field of the transmitted light with p - and s -polarized components E_{tp}, E_{ts} [22]:

$$\begin{pmatrix} E_{tp} \cos \theta_2 \\ n_2 E_{tp} \\ E_{ts} \\ n_2 E_{ts} \cos \theta_2 \end{pmatrix} = \begin{pmatrix} P_{11} & P_{12} & P_{13} & P_{14} \\ P_{21} & P_{22} & P_{23} & P_{24} \\ P_{31} & P_{32} & P_{33} & P_{34} \\ P_{41} & P_{42} & P_{43} & P_{44} \end{pmatrix} \begin{pmatrix} (E_{ip} - E_{rp}) \cos \theta_0 \\ n_0 (E_{ip} + E_{rp}) \\ (E_{is} + E_{rs}) \\ n_0 (E_{is} - E_{rs}) \cos \theta_0 \end{pmatrix}. \quad (33)$$

Here, n_2 is the refractive index of the ambient medium at the second side of the film (opposed to the side facing the incident beam) and θ_2 is the corresponding angle of the transmitted beam to the film normal. In our case of a freely suspended smectic film we have, of course, $n_2 = n_0$ and $\theta_2 = \theta_0$. When P is known, the reflection and transmission matrices R and T , from which the ellipsometric quantities Δ and Ψ of the reflected and transmitted light are obtained, can be calculated. In the four equations represented by (33) one can eliminate, *e.g.*, first the components of the transmitted field, obtaining two equations for the reflected field which can be written as [22]:

$$\begin{pmatrix} E_{rp} \\ E_{rs} \end{pmatrix} = \begin{pmatrix} R_{pp} & R_{ps} \\ R_{sp} & R_{ss} \end{pmatrix} \begin{pmatrix} E_{ip} \\ E_{is} \end{pmatrix}, \quad (34)$$

with

$$R_{pp} = (a_{ip}b_{rs} - a_{rs}b_{ip})/(a_{rs}b_{rp} - a_{rp}b_{rs}), \quad (35)$$

$$R_{ps} = (a_{is}b_{rs} - a_{rs}b_{is})/(a_{rs}b_{rp} - a_{rp}b_{rs}), \quad (36)$$

$$R_{sp} = (a_{rp}b_{ip} - a_{ip}b_{rp})/(a_{rs}b_{rp} - a_{rp}b_{rs}), \quad (37)$$

$$R_{ss} = (a_{rp}b_{is} - a_{is}b_{rp})/(a_{rs}b_{rp} - a_{rp}b_{rs}), \quad (38)$$

$$a_{ip} = (P_{12}n_2 - P_{22} \cos \theta_2)n_0 + (P_{11}n_2 - P_{21} \cos \theta_2) \cos \theta_0, \quad (39)$$

$$a_{rp} = (P_{12}n_2 - P_{22} \cos \theta_2)n_0 \quad (40)$$

$$- (P_{11}n_2 - P_{21} \cos \theta_2) \cos \theta_0,$$

$$a_{is} = (P_{13}n_2 - P_{23} \cos \theta_2) \quad (41)$$

$$+ (P_{14}n_2 - P_{24} \cos \theta_2)n_0 \cos \theta_0,$$

$$a_{rs} = (P_{13}n_2 - P_{23} \cos \theta_2) \quad (42)$$

$$- (P_{14}n_2 - P_{24} \cos \theta_2)n_0 \cos \theta_0,$$

$$b_{ip} = (P_{32}n_2 \cos \theta_2 - P_{42})n_0 \quad (43)$$

$$+ (P_{31}n_2 \cos \theta_2 - P_{41}) \cos \theta_0,$$

$$b_{rp} = (P_{32}n_2 \cos \theta_2 - P_{42})n_0 \quad (44)$$

$$- (P_{31}n_2 \cos \theta_2 - P_{41}) \cos \theta_0,$$

$$b_{is} = (P_{33}n_2 \cos \theta_2 - P_{43})n_0 \quad (45)$$

$$+ (P_{34}n_2 \cos \theta_2 - P_{44})n_0 \cos \theta_0,$$

$$b_{rs} = (P_{33}n_2 \cos \theta_2 - P_{43})n_0 \quad (46)$$

$$- (P_{34}n_2 \cos \theta_2 - P_{44})n_0 \cos \theta_0.$$

With these results for the reflection matrix R one can go back to (33) and obtain the elements of the transmission matrix T :

$$T_{pp} = [P_{21} \cos \theta_0 + P_{22}n_0 + R_{pp}(P_{22}n_0 - P_{21} \cos \theta_0) + R_{sp}(P_{23} - P_{24}n_0 \cos \theta_0)]/n_2, \quad (47)$$

$$T_{ps} = [P_{23} + P_{24}n_0 \cos \theta_0 + R_{ps}(P_{22}n_0 - P_{21} \cos \theta_0) + R_{ss}(P_{23} - P_{24}n_0 \cos \theta_0)]/n_2, \quad (48)$$

$$T_{sp} = P_{31} \cos \theta_0 + P_{32}n_0 + R_{pp}(P_{32}n_0 - P_{31} \cos \theta_0) + R_{sp}(P_{33} - P_{34}n_0 \cos \theta_0), \quad (49)$$

$$T_{ss} = P_{33} + P_{34}n_0 \cos \theta_0 + R_{ps}(P_{32}n_0 - P_{31} \cos \theta_0) + R_{ss}(P_{33} - P_{34}n_0 \cos \theta_0). \quad (50)$$

The ellipsometric quantities Δ and Ψ , which we want to compare with our measured values, are then obtained by equations (2) and (3).

References

1. Ch. Bahr, *Int. J. Mod. Phys. B* **8**, 3051 (1994).
2. T. Stoebe, C.C. Huang, *Int. J. Mod. Phys. B* **9**, 2285 (1995).
3. R.B. Meyer, L. Liebert, L. Strzelecki, P. Keller, *J. Phys. Lett.* **36**, L69 (1975).
4. C.Y. Young, R. Pindak, N.A. Clark, R.B. Meyer, *Phys. Rev. Lett.* **40**, 773 (1978).
5. C. Rosenblatt, R. Pindak, N.A. Clark, R.B. Meyer, *Phys. Rev. Lett.* **42**, 1220 (1979).
6. S. Heinekamp, R.A. Pelcovits, E. Fontes, E.Y. Chen, R. Pindak, R.B. Meyer, *Phys. Rev. Lett.* **52**, 1017 (1984).
7. S.M. Amador, P.S. Pershan, *Phys. Rev. A* **41**, 4326 (1990).
8. Ch. Bahr, C.J. Booth, D. Fliegner, J.W. Goodby, *Phys. Rev. E* **52**, R4612 (1995).
9. Ch. Bahr, C.J. Booth, D. Fliegner, J.W. Goodby, *Phys. Rev. Lett.* **77**, 1083 (1996).
10. R.B. Meyer, *Phys. Rev. Lett.* **22**, 918 (1969).
11. P.O. Andreeva, V.K. Dolganov, K.P. Meletov, *JETP Lett.* **66**, 443 (1997).

12. P. Pieranski, L. Beliard, J.-Ph. Tournellec, X. Leoncini, C. Furtlehner, H. Dumoulin, E. Riou, B. Jouvin, J.-P. Fénerol, Ph. Palaric, J. Heuving, B. Cartier, I. Kraus, *Physica A* **194**, 364 (1993).
13. Ch. Bahr, D. Fliegner, *Phys. Rev. A* **46**, 7657 (1992).
14. Below the bulk Sm-A – Sm-C transition temperature a small difference between Ψ_+ and Ψ_- occurs. The reason might consist of slight variations of ϕ across the film which are the remains of the helical structure of the bulk Sm-C phase of chiral molecules.
15. S. Teitler, B. Henvis, *J. Opt. Soc. Am.* **60**, 830 (1970).
16. D.W. Berreman, *J. Opt. Soc. Am.* **62**, 502 (1972).
17. K. Binder, *Phase Transitions and Critical Phenomena*, edited by C. Domb, J.L. Lebowitz (Academic, London 1986), Vol. 8.
18. R. Geer, T. Stoebe, C.C. Huang, *Phys. Rev. E* **48**, 408 (1993).
19. P.G. de Gennes and J. Prost, *The Physics of Liquid Crystals* (Oxford University Press, Oxford, 1993), p. 137.
20. For MB8OBC, however, an odd behavior of the Δ values near the surface was observed in medium thick films (see [8]) which may result from a distortion of the S-structure by a small flexoelectric polarization.
21. D. Schlauf, Ch. Bahr, C.C. Huang, J.W. Goodby, *Ferroelectrics* **212**, 221 (1998).
22. R.M.A. Azzam, N.M. Bashara, *Ellipsometry and Polarized Light* (North Holland, Amsterdam, 1989), pp. 340-352.
23. H. Wöhler, G. Haas, M. Fritsch, D.A. Mlynski, *J. Opt. Soc. Am. A* **5**, 1554 (1988).